Separation of Azeotropic Mixtures using Protic Ionic Liquids as Extraction Solvents

Julio E. Sosa[a,b]*, João M. M. Araújo*[a]*, Eliseo Amado-González*[b] *and Ana B. Pereiro*[a,*]

[a] LAQV, REQUIMTE, Departamento de Química, Faculdade de Ciências e Tecnologia, Universidade Nova de Lisboa (FCT NOVA), 2829-516 Caparica, Portugal. (je.parra@campus.fct.unl.pt, J.E.S.; jmmda@fct.unl.pt, J.M.M.A.)

[b] Faculty of Basic Sciences, University of Pamplona, Biofuels Lab-IBEAR, Pamplona, Colombia (eamado@unipamplona.edu.co, E.A-G.)

* Correspondence to: A.B. Pereiro., E-mail: anab@fct.unl.pt; Fax: (+351) 212948550; Tel: (+351) 212948318.

Abstract

The aim of this work is to evaluate the separation of hydrocarbons (hexane and heptane) from their azeotropic mixtures with ethanol using protic ionic liquid (PIL) as extraction solvents. With this goal in mind, PILs were synthesized and their thermal and physical characterization were carried out. Experimental determination of the phase equilibrium for the ternary systems hydrocarbons + ethanol + PIL at 298.15 K and 101.2 kPa were also carried out in order to evaluate the feasibility of this application. The solute distribution ratio and the selectivity were also determined to compare the solvent capacity of these PILs. The NRTL equation was used to correlate the experimental data. Furthermore, this paper provides a comparison of the solvent capacity of these PILs with different extraction solvents (ionic liquids (ILs), ILs mixtures and deep eutectic solvents) available in the literature. Then, a critical review for the separation of these azeotropic mixtures was carried out using the extraction processes data obtained through the simulation using a conventional software.

Keywords: Liquid-liquid equilibria; Protic ionic liquids; Azeotropic mixtures; Extraction processes.

1. Introduction

In many areas of industry, the increasing interest related to development of green processes and products makes ionic liquids (ILs) candidates to replace conventional organic solvents in many chemical processes [1]. The possibility of recovering compounds used in industrial processes is not easy, because in many cases the mixtures can form azeotropes [2]. The separation of these azeotropic mixtures into the neat components is needed so that they can be reused, minimizing the costs of industrial processes. Extractive and azeotropic distillation are the most widely separation processes used to remove one of the components in the azeotropic system. In this work liquid–liquid separation was selected because it is an advantageous alternative to reduce the energy consumption and the environmental impact of these conventional processes.

Ionic liquids are widely recognized as green alternatives for engineers not only due to their negligible vapor pressure at room temperature but also for their recyclability [3,4]. Moreover, ILs can be easily tuned to obtain the appropriated properties for the chemical engineering needs in terms of efficiency and cost of the processes [5]. However, since conventional ILs (aprotic ILs) are expensive due to their complex synthesis procedures, the possibility of obtaining ILs from cheap precursors and simple synthesis processes, place the protic ionic liquids (PILs) as a great alternative to traditional ILs [6,7]. These PILs combine excellent properties, such as their high conductivity and exceptional electrochemical properties [7]. Moreover, these compounds present one or more labile hydrogen atoms (in the cationic species) that allow the presence the strong hydrogen bonding interactions. These properties are very interesting in extraction solvents because it can enhance the separation capacity of these compounds. Recently, PILs, like 2-hydroxyethylamonium formate, have received a great attention due to the low costs of synthesis, environmentally friendly nature and suitable solvation properties [8-9].

In petrochemical industry, there are several processes where hydrocarbons (hexane or heptane) and ethanol are present to produce oxygenated additives, reducing the lead in gasoline [10-19]. These compounds form azeotropic mixtures that are conventionally separated using azeotropic distillation [20,21], pervaporation [22], and reverse osmosis [23]. In this paper, PILs based on 2-hydroxyethylamonium cation combined with different carboxylate-based anions were synthetized and characterized in order to be used as extraction solvents for the removal of hydrocarbons (hexane or heptane) from its azeotropic mixtures with ethanol. Experimental liquid-liquid equilibrium (LLE) for the ternary systems hydrocarbons + ethanol + PILs were determined as a continuation of our study for the separation of these azeotropic mixtures [10-19,23]. The PILs capacity to separate these azeotropic mixtures was evaluated using the solute distribution ratio and the selectivity. Furthermore, experimental LLE data were successfully correlated using the NRTL equation [23,24]. This correlation eases the implementation and use of this model in the simulation studies for extraction processes. Finally, Aspen Hysys software was used to optimize the operation conditions for a continuous countercurrent extraction process for the separation of hydrocarbons (hexane or heptane) from its azeotropic mixture with ethanol. The separation capacity of PILs is compared to the capacity of other ILs, ILs mixtures and deep eutectic solvents (DESs) from a critical review of the literature [10-18, 23,25-37].

2. Experimental Section

2.1. Materials

The chemicals and reagents used in this work are shown in Table S1 of Supporting Information (SI) together with the corresponding suppliers and purities. The PILs used in this work were synthesized by a Brønsted-Lowry titration between ethanolamine and the corresponding organic acid (see Table S1 of SI) and were purified as described in literature [8,38]. PILs were dried under vacuum (4 Pa) for at least 48 h with continuous stirring. Karl Fisher (KF) titration (Methonm Ion analysis 831 KF Coulometer) was used to calculate the water content and the results show values less than 1500 ppm. The PILs purities were verified by ^{1}H NMR (Bruker AVANCE 400 spectrometer). All compounds obtained a purity higher than 98 % in mass fraction. The chemical structures of these compounds are presented in Table S2 of SI.

The ^{1}H NMR characterization obtained for each PIL was the following: $[N_{0002(OH)}][HCO_2]$ δ_H (400 MHz; DMSO) 8.41 (1H, s, *H*-COO-), 5.97-4.37 (3H, broad signal, NH_3^+), 3.57 (2H, t, N-CH_2-), 2.83 (2H, t, -CH_2-O); $[N_{0002(OH)}][C_2H_5CO_2]$ δ_H (400 MHz; D_2O) 3.72 (2H, t, CH_2-O), 3.04 (2H, t, N-CH_2), 2.09 (2H, q, CH_3-CH_2-COO^-), 0.96 (3H, t, CH_3-CH_2-); $[N_{0002(OH)}][C_3H_7CO_2]$ δ_H (400 MHz; D_2O) 3.74 (2H, t, -CH_2-O); 3.06 (2H, t, N-CH_2-); 2.07 (2H, t, -CH_2-COO^-); 1.48 (2H, q, CH_3-CH_2-CH_2-); 0.81 (3H, t, CH_3-CH_2-).

2.2. Thermal Analysis

The decomposition temperatures of the pure $[N_{0002(OH)}][HCO_2]$, $[N_{0002(OH)}][C_2H_5CO_2]$ and $[N_{0002(OH)}][C_3H_7CO_2]$ were determined in a thermogravimetric analyser (LABSYS Evo STA). The experiments were performed at atmospheric pressure in platinum pans with heating rates of 1 $K \cdot min^{-1}$. The onset temperature (T_{onset}), starting temperature (T_{start}) and decomposition temperature (T_{dec}) were determined and correspond to the temperatures at which the baseline slope changed during heating, the weight loss was less than 1%, and the weight loss was 50%, respectively. Duplicates were done and the uncertainty was better than 2 K.

The melting points of the ionic liquids were measured by differential scanning calorimetry using a DSC Q500 (TA Instruments, calibrated with indium standard). Dry nitrogen at a flow rate of about 50 $cm^3 \cdot min^{-1}$ was used as the purge gas of the DSC cell. The samples were cooled until 183.15 K, then held during 30 min in isotherm, and heated up to 373.15 K for $[N_{0002(OH)}][HCO_2]$, up to 336.15 K for $[N_{0002(OH)}][C_2H_5CO_2]$ and up to 349.15 K for $[N_{0002(OH)}][C_3H_7CO_2]$. This procedure was repeated three times at different rates (10 $K \cdot min^{-1}$, 5 $K \cdot min^{-1}$ and 1 $K \cdot min^{-1}$). At the same rate, the results from the second and subsequent cycles were reproducible. The results were analysed using the software Universal Analysis (TA instruments) software. The melting temperature (T_m), solid-solid transitions (T_s) and glass transitions (T_g) were determined. Duplicates were done and the uncertainty was better than 1 K.

2.3. Density, Dynamic Viscosity and Refractive Index

The density and dynamic viscosity of the pure $[N_{0002(OH)}][HCO_2]$ were measured in an SVM 3000 Anton Paar rotational Stabinger viscometer operating at atmospheric pressure in the temperature range from 283.15 K to 343.15 K. Duplicates were done and the reported data are the average value with a maximum relative standard deviation of 1% for viscosity measurements and an uncertainty of the density better than 0.0002 $g \cdot cm^{-3}$. The global uncertainty of the measurements, considering the purity and the sample handling, is estimated to be 0.1% for the density and 2% for the viscosity.

The refractive index of $[N_{0002(OH)}][HCO_2]$ was determined using the automatic ABBEMAT 500 Anton Paar refractometer, with an uncertainty in the experimental measurements of ± 4.10^{-5}. Reference fluids (water mili-Q and tetrachlorethylene) were routinely used for the calibration. The verification of the calibration was carried out before each series of measurements in all equipments.

2.4. Liquid-Liquid Equilibrium (LLE) Measurements

Ternary LLE data were measured in a glass cell containing a magnetic stirrer with a water jacket connected to a bath controlled at 298.15 K. The temperature in the glass cell was determined by a thermometer with an uncertainty of ± 0.01 K. For the LLE measurements, 12 ml of a ternary mixture of known composition was added to this glass cell and was stirred vigorously for 1 h and left to settle for 12 h. Preliminary tests showed that this time was enough to guarantee that the thermodynamic equilibrium was achieved. Then, samples of both layers were taken with a syringe and the refractive index of these samples were measured. Finally, the compositions of both phases in equilibrium were calculated using the fitting of the refractive index data (calibration curves previously constructed at 298.15 K) with the composition along the binodal curve using the following equations [10]:

$$n_D = A\cdot w_1 + B\cdot w_1^2 + C\cdot w_1^3 + D\cdot w_1^4 + E\cdot w_2 + F\cdot w_2^2 + G\cdot w_2^3 + H\cdot w_2^4 + I\cdot w_3 + J\cdot w_3^2 + K\cdot w_3^3 + L\cdot w_3^4 \quad (1)$$

$$w_3 = M \exp\left[(N\cdot w_1^{0.5}) - (O\cdot w_1^3)\right] \quad (2)$$

$$w_3 = 1 - (w_1 + w_2) \quad (3)$$

where n_D corresponds to refractive index, A to O are the adjustable parameters, and w_1, w_2 and w_3 are the mass fraction compositions of hydrocarbon, ethanol and PIL, respectively. The quality of the calibration curves was checked with samples of the binodal curves and the uncertainty of the phase composition is better than 0.005 in mass fraction. These curves were obtained after the determination of the binodal curve. These binodal curves were detected visually using known masses of the three components in a glass cell. Then, ethanol was added slowly until one phase was obtained. All measurements were performed with an uncertainty of $\pm 10^{-4}$ in mass fraction.

2.4. Solid-Liquid Equilibrium (SLE) Measurements

The solid-liquid equilibria were determined using a dynamic method with visual detection of the phase transition. Ternary mixtures were prepared using an analytical high-precision balance with ± 0.01 mg resolution in a glass cell containing a magnetic stirrer. This glass cell has a water jacket connected to a bath which is controlled at 298.15 K (with an accuracy of ± 0.01 K). The SLE was determined using these known quantities of the three components in the immiscible region where known quantities of ethanol were slowly added maintaining the stirring until the last crystal disappears. The uncertainty of the phase compositions is better than ± 0.006 in mass fraction.

3. Results and Discussion

3.1. Characterization of Protic Ionic Liquids

The decomposition temperatures and melting points of the pure PILs synthesized in this work determine the range of application of these compounds. The results presented in Table 1 suggest that the increment of the hydrogenated alkyl chain length on the anion causes an increment on the melting temperature. Only $[N_{0002(OH)}][HCO_2]$ is liquid at room temperature and presents the highest decomposition temperature (although the differences in this thermal property are not significant). The melting temperatures of $[N_{0002(OH)}][C_2H_5CO_2]$ and $[N_{0002(OH)}][C_3H_7CO_2]$ were not determined because are close or higher than their decomposition temperatures. Finally, the glass transitions were only detected for $[N_{0002(OH)}][C_2H_5CO_2]$ and $[N_{0002(OH)}][C_3H_7CO_2]$ at similar temperatures, close to 208 K.

Table 1

Thermal properties[a] of the pure ionic liquids $[N_{0002(OH)}][HCO_2]$, $[N_{0002(OH)}][C_2H_5CO_2]$ and $[N_{0002(OH)}][C_3H_7CO_2]$ studied in this work.

Ionic Liquid	T_{start} / K	T_{onset} / K	T_{dec} / K	T_m /K	T_s / K	T_g / K
$[N_{0002(OH)}][HCO_2]$	389	483	486	278	192	
$[N_{0002(OH)}][C_2H_5CO_2]$	346	431	432			209
$[N_{0002(OH)}][C_3H_7CO_2]$	359	434	436			207

[a]Standard uncertainties of the temperature was ± 2 K.

Thermophysical properties (density, viscosity and refractive index) of $[N_{0002(OH)}][HCO_2]$ were determined between 283.15 and 343.15 K and are reported in Table 2. A comparison with the data available in the literature is illustrated in Fig. S1 of SI [8,9,39-44]. Although there are several experimental data for $[N_{0002(OH)}][HCO_2]$, it should be stated that the results are very different. These differences can be related to the different purities (water or unreacted chemicals) of the used ionic liquids. However, the experimental results determined in this work are similar to the reported by Ghatee et al. [41]. These studies are important because there is a lack of accuracy of the most common reported methods and a limited range of temperatures are studied which is a barrier for the industrial application of ionic liquids.

Table 2

Density, ρ, dynamic viscosity, η, and refractive index, n_D, of the pure $[N_{0002(OH)}][HCO_2]$ at 101 kPa.[a]

T/K	ρ/g cm^{-3}	η/mPa·s	n_D
283.15	1.2116	485.6	1.47040
288.15	1.2090	344.3	1.46941
293.15	1.2065	249.4	1.46841
298.15	1.2041	184.8	1.46743
303.15	1.2017	140.0	1.46645

308.15	1.1994	108.2	1.46549
313.15	1.1971	85.12	1.46454
318.15	1.1948	68.04	1.46357
323.15	1.1925	55.18	1.46260
328.15	1.1902	45.37	1.46166
333.15	1.1882	37.76	1.46078
338.15	1.1854	31.77	1.45986
343.15	1.1829	27.01	1.45894

[a] Standard uncertainty, u, for pressure, temperature, density, viscosity and refractive index were: $u(P) = 0.5$ kPa; $u(T) = 0.02$ K, $u(\rho)$: 0.0002 $g\cdot cm^{-3}$, $u(\eta)$: 1% $u(n_D)$: 0.00004

3.2. Ternary Diagrams

Phase equilibria data for ternary systems hexane (1) + ethanol (2) + PIL (3) or heptane (1) + ethanol (2) + PIL (3) obtained at 298.15 K are presented in Tables S3 and S4 of SI. The tables include liquid-liquid and solid-liquid equilibrium data, respectively, and these data are also plotted in Fig. 1 (comparison of all systems). SLE regions for ternary systems with hexane and heptane are found for the ionic liquids $[N_{0002(OH)}][C_2H_5CO_2]$ and $[N_{0002(OH)}][C_3H_7CO_2]$. The binodal curves represent the size and shape of the LLE region of these systems. A comparison of these curves shows a slight increase of the immiscible region in the heptane-based systems. The same behaviour is observed when we compare the SLE regions. Moreover, it can be observed that the binodal curve decreases when the length of the alkyl chain in the anion increases. Fig. 1 also represents a clear visualization of the global composition in the different heterogeneous regions. The results show that these PILs are practically immiscible in the hydrocarbons herein tested (hexane and heptane). Furthermore, the composition of ethanol is low in the hydrocarbon rich phase of every studied system. Finally, the positive slopes for the experimental tie lines in all systems suggest that the extraction of ethanol is always possible from their mixture with the hydrocarbon in both systems.

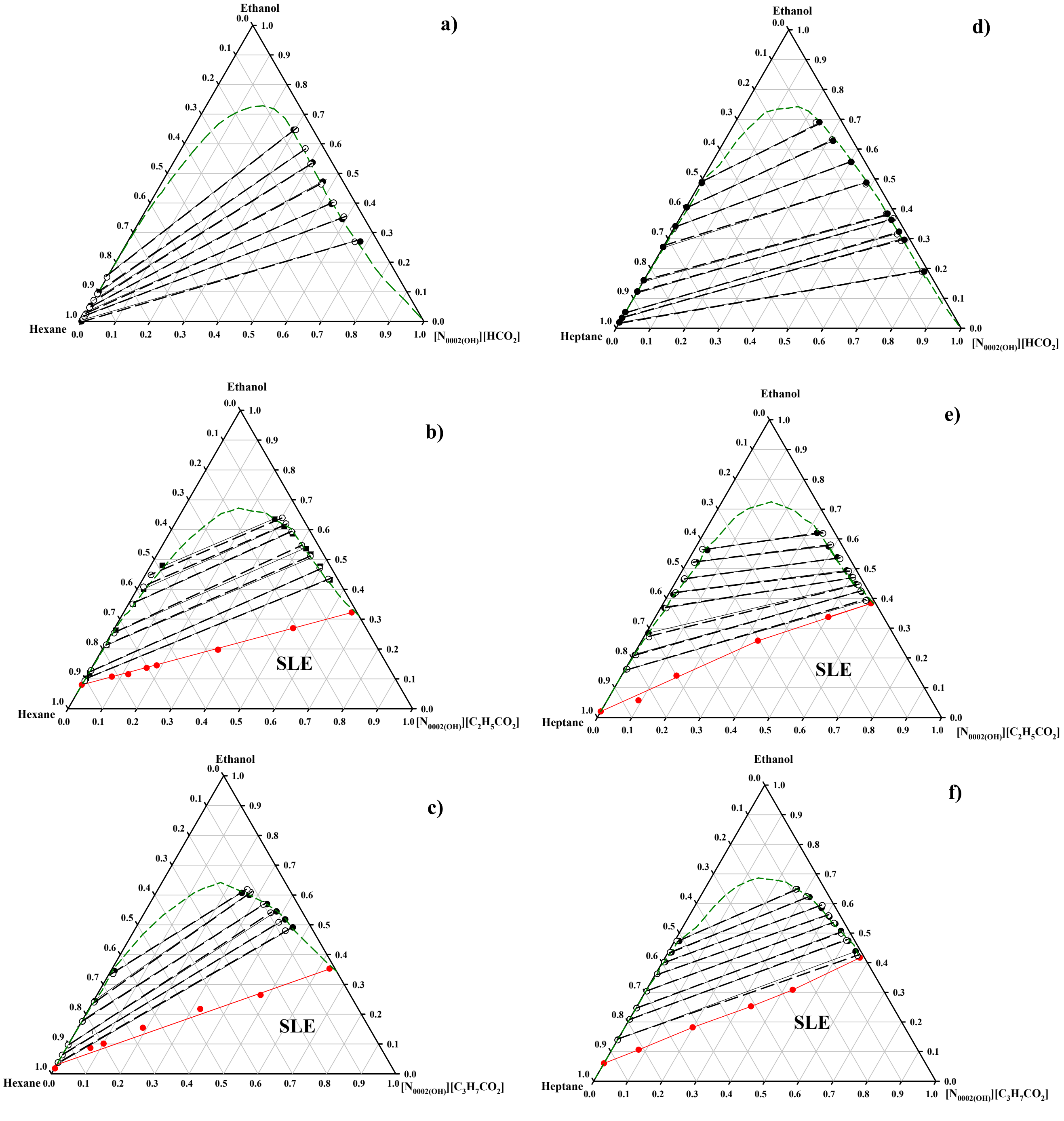

Fig. 1. Triangular phase diagram for ternary system in molar fraction: a) hexane (1) + ethanol (2) + $[N_{0002(OH)}][HCO_2]$ (3); b) hexane (1) + ethanol (2) + $[N_{0002(OH)}][C_2H_5CO_2]$ (3); c) hexane (1) + ethanol (2) + $[N_{0002(OH)}][C_3H_7CO_2]$ (3); d) heptane (1) + ethanol (2) + $[N_{0002(OH)}][HCO_2]$ (3); e) heptane (1) + ethanol (2) + $[N_{0002(OH)}][C_2H_5CO_2]$ (3); f) heptane (1) + ethanol (2) + $[N_{0002(OH)}][C_3H_7CO_2]$ (3) at 298.15 K where (● and —) are the experimental LLE data; (○ and — —) are the NRTL correlation; (● and —) are the experimental SLE data; and (----) are the experimental data of the binodal curve.

3.3. Distribution Coefficient and Selectivity

The distribution coefficient or solute distribution ratio (β) shows the ratio between the amount of ethanol extracted to the IL rich phases and the amount of remained in the hydrocarbon rich phase. Then, this parameter is related to the solvent capacity of the PILs and determines the amount of compound required for the extraction process. The selectivity, S, the parameter that evaluates the efficiency of the extraction solvent, in this case the extraction of ethanol, from its azeotropic mixture with the inert, in this case hydrocarbon (hexane or heptane). This selectivity is based on previously calculated β values and provides the number of equilibrium stages needed in the separation unit (if the selectivity has high values, less equilibrium stages are needed for the separation process). These parameters are widely used in assessing the separation power of different extraction solvents in liquid-liquid extraction processes and are defined by the following expressions:

$$\beta = \frac{x_2^{\mathrm{II}}}{x_2^{\mathrm{I}}} \tag{4}$$

$$S = \left(\frac{x_1^{\mathrm{I}}}{x_1^{\mathrm{II}}}\right) \cdot \left(\frac{x_2^{\mathrm{II}}}{\mathrm{x}_2^{\mathrm{I}}}\right) \tag{5}$$

where x represents the molar fraction, subscripts 1 and 2 are the hydrocarbon and the ethanol, respectively, and superscripts I and II indicate the hydrocarbon rich phase (upper phase) and in the IL rich phase (lower phase), respectively. The results are reported in Table S3 of SI and Fig. 2 depicts the values obtained for the studied ternary systems at 298.15 K. In both cases, the β and S values decrease with the increment of the ethanol concentration in the hydrocarbon rich phase.

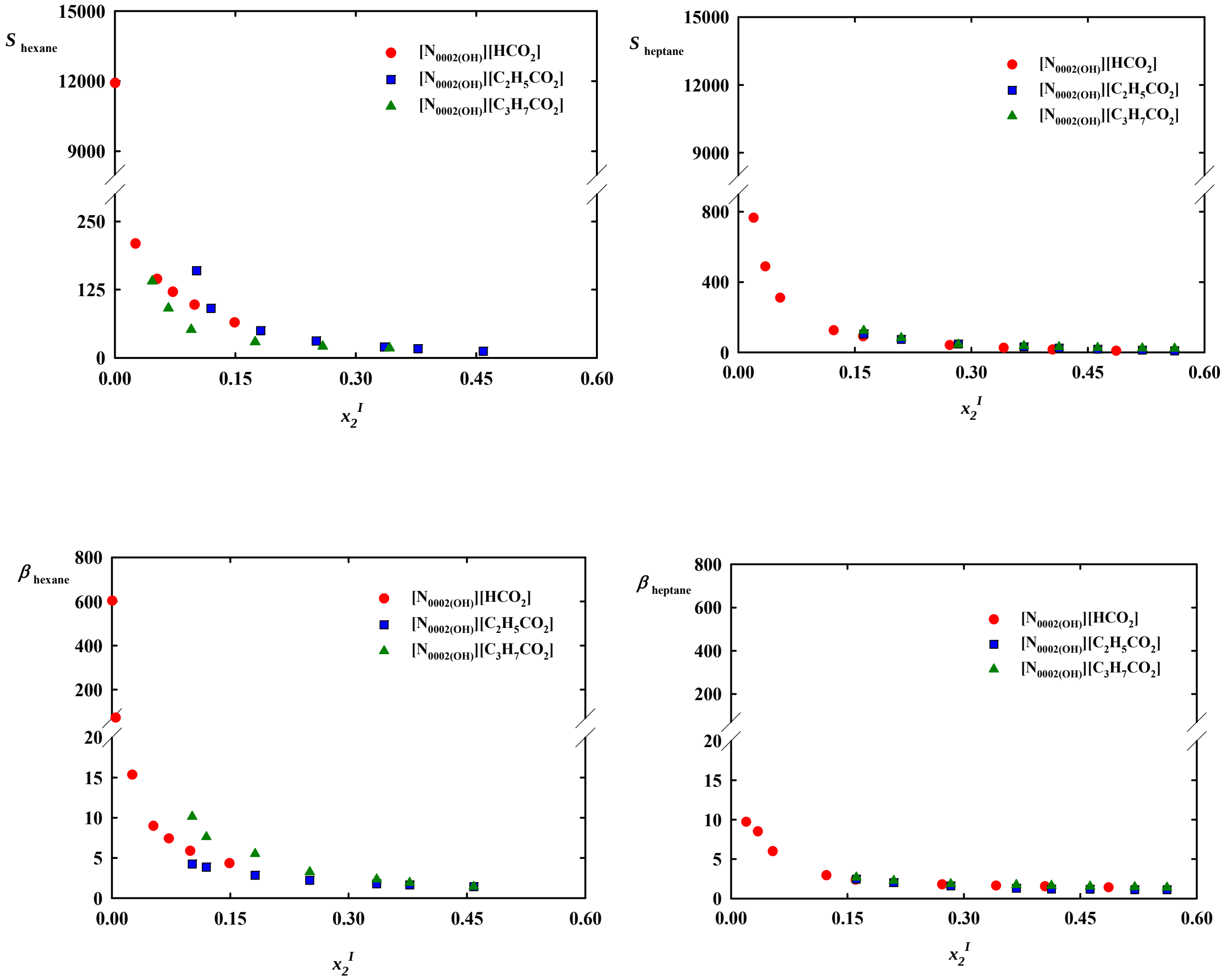

Fig. 2. Distribution coefficients (*β*). Selectivity (*S*) versus molar fraction of ethanol in the hydrocarbon phase for the system hydrocarbon (1) + ethanol (2) + PIL (3) at 298.15 K for: ● $[N_{0002(OH)}][HCO_2]$; ■ $[N_{0002(OH)}][C_2H_5CO_2]$; ▲ $[N_{0002(OH)}][C_3H_7CO_2]$.

Fig. 2 and Table S3 of SI show not significant difference in these parameters obtained for the systems hydrocarbon + ethanol + PIL meaning that there is no a clear effect due to these anions differences. However, small differences suggest that $[N_{0002(OH)}][HCO_2]$ has the best capacity to extract ethanol from its mixture with hydrocarbon. It was found higher differences to compositions lower than 0.1, suggesting better results for $[N_{0002(OH)}][HCO_2]$. These high values may be due to the higher interaction between the –OH group of ethanol with the $[N_{0002(OH)}][HCO_2]$ ionic liquid.

The other two PILs, $[N_{0002(OH)}][C_2H_5CO_2]$ and $[N_{0002(OH)}][C_3H_7CO_2]$, cannot be used in this range of compositions because they are in the SLE region.

3.4. Correlation using NRTL model

In order to perform the simulation studies and process design for the extraction processes, the LLE data must be fitted to a thermodynamic model. Following the methodology widely used for ILs [16,45], NRTL (Non Random Two Liquid) model was applied to these partially miscible systems. This model has already demonstrated its ability to satisfactory describe the LLE behaviour of systems involving ILs [16,45]. The third randomness parameter α was optimized and their values are reported in Table 3. The determination of the binary parameters of NRTL was adjusted to minimize the difference between the experimental and the calculated mole fraction defined as:

$$O.F. = \min \sum_{l=1}^{\mathrm{nt}} \sum_{i=1}^{\mathrm{nc}} \left[\left[\left(x_{il}^{\mathrm{I}}(exp) - x_{il}^{\mathrm{I}}(calc) \right)^2 \right] + \left[\left(x_{il}^{\mathrm{II}}(exp) - x_{il}^{\mathrm{II}}(calc) \right)^2 \right] \right] \tag{6}$$

where: *x* is the mole fraction; *exp* and *calc* are the experimental and calculated values, respectively; subscripts *i* and *l* refer to each component and the tie-line, respectively; nc and nt are the total number of components and tie-lines, respectively; and superscripts I and II indicate the hydrocarbon and the IL rich phases, respectively. The NRTL fitting parameters are shown in Table 3 and the consistency of these sets of parameters have been verified (satisfied the Gibbs stability criteria and the isoactivity criterion [46-48]). In this table, the corresponding deviation, RMSD, is also shown which was calculated by applying the following expression:

$$\mathrm{RMSD} = \left(\frac{\sum_i \left(x_{ilm}^{\mathrm{exp}} - x_{ilm}^{\mathrm{calc}} \right)^2}{6k} \right)^{1/2} \tag{7}$$

where the subscripts *i*, *l* and *m* are the component, the phase and the tie–line, respectively. The *k* value indicates the number of experimental tie-lines.

The RMSD values are lower than 0.020 for the ternary systems hydrocarbon (1) + ethanol (2) + PIL (3). A comparison between the experimental data and those obtained from the NRTL equation is illustrated in Fig. 1 where the NRTL model describes the liquid-liquid behaviour of the studied mixtures.

This paper also provides a critical review on the separation power of the different extraction solvents used in the literature [10-18, 25-37] for the azeotropic mixtures studied in this work. The literature review on extraction solvents is summarized in Table S5 of SI where can be verified the great diversity of ILs, deep eutectic solvents (DESs) and mixtures that have been studied. In order to include these solvents in the simulation studies, new NRTL parameters were calculated for all ternary systems and are summarized in Table S6 of SI. A comparison between the deviations calculated in the literature (see equations in SI) and the RMSDs determine in this work is plotted in Fig. 3 and listed in Table S6 of SI. In general, the NRTL fitting parameters calculated in this work describe better the phase equilibria behaviour of these ternary systems.

Table 3.
NRTL parameters obtained for the ternary system hydrocarbon (1) + ethanol (2) + ionic liquid (3).

ij	$\frac{\Delta g_{ij}}{J.mol^{-1}}$	$\frac{\Delta g_{ji}}{J.mol^{-1}}$	α	RMSD
Hexane (1) + Ethanol (2) + [$N_{0002(OH)}$][HCO_2] (3)				
12	1435.1	189.72	0.10	
13	5974.9	-265.59	0.10	0.007
23	2291.8	-2291.9	0.10	
Hexane (1) + Ethanol (2) + [$N_{0002(OH)}$][$C_2H_5CO_2$] (3)				
12	381.23	1022.7	0.28	
13	4347.1	1124.1	0.10	0.012
23	-981.15	1815.7	0.10	
Hexane (1) + Ethanol (2) + [$N_{0002(OH)}$][$C_3H_7CO_2$] (3)				
12	916.57	615.79	0.29	
13	4455.5	-425.63	0.09	0.010
23	4254.9	-2269.1	0.10	
Heptane (1) + Ethanol (2) + [$N_{0002(OH)}$][HCO_2] (3)				
12	884.55	-185.72	0.15	
13	6610.7	-355.59	0.10	0.004
23	4574.1	-2991.9	0.10	
Heptane (1) + Ethanol (2) + [$N_{0002(OH)}$][$C_2H_5CO_2$] (3)				
12	-48.088	1297.8	0.10	
13	3965.4	1202.1	0.10	0.007
23	218.34	869.62	0.29	
Heptane (1) + Ethanol (2) + [$N_{0002(OH)}$][$C_3H_7CO_2$] (3)				
12	-2188.7	-175.72	0.28	
13	5258.1	-395.59	0.10	0.005
23	674.04	-5141.1	0.10	

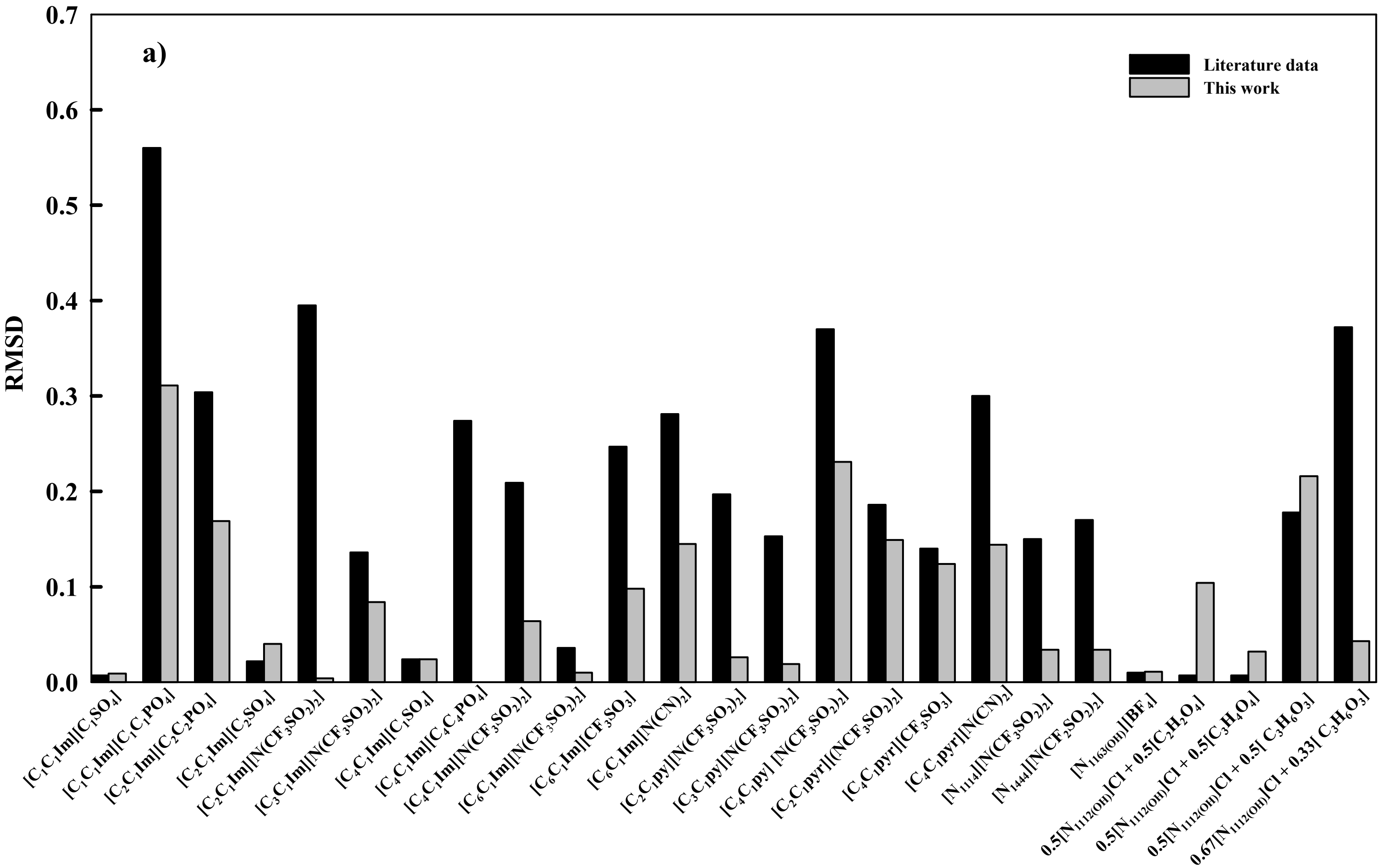
a)
Literature data
This work
RMSD
0.7
0.6
0.5
0.4
0.3
0.2
0.1
0.0
$[C_1C_1Im][C_1SO_4]$
$[C_1C_1Im][C_1C_1PO_4]$
$[C_2C_1Im][C_2C_2PO_4]$
$[C_2C_1Im][C_2SO_4]$
$[C_2C_1Im][N(CF_3SO_2)_2]$
$[C_3C_1Im][N(CF_3SO_2)_2]$
$[C_4C_1Im][C_1SO_4]$
$[C_4C_1Im][C_4C_4PO_4]$
$[C_4C_1Im][N(CF_3SO_2)_2]$
$[C_6C_1Im][N(CF_3SO_2)_2]$
$[C_6C_1Im][CF_3SO_3]$
$[C_6C_1Im][N(CN)_2]$
$[C_2C_1py][N(CF_3SO_2)_2]$
$[C_3C_1py][N(CF_3SO_2)_2]$
$[C_4C_1py] [N(CF_3SO_2)_2]$
$[C_2C_1pyr][(NCF_3SO_2)_2]$
$[C_4C_1pyr][CF_3SO_3]$
$[C_4C_1pyr][N(CN)_2]$
$[N_{1114}][N(CF_3SO_2)_2]$
$[N_{1444}][N(CF_2SO_2)_2]$
$[N_{1163(OH)}][BF_4]$
$0.5[N_{1112(OH)}]Cl + 0.5[C_2H_2O_4]$
$0.5[N_{1112(OH)}]Cl + 0.5[C_3H_4O_4]$
$0.5[N_{1112(OH)}]Cl + 0.5[C_3H_6O_3]$
$0.67[N_{1112(OH)}]Cl + 0.33[C_3H_6O_3]$

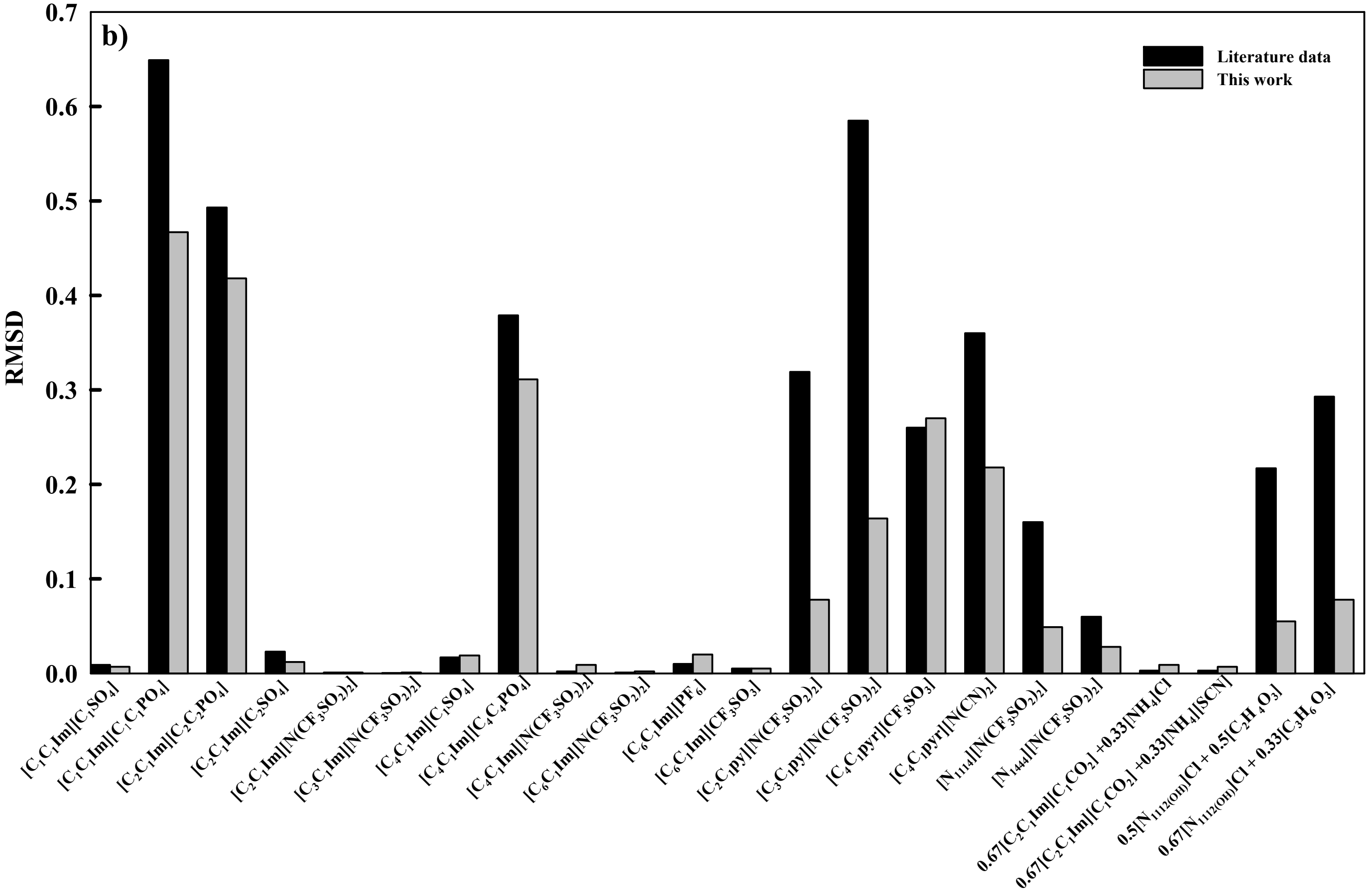

Fig. 3. Deviation calculated from NRTL correlations for the ternary systems: a) hexane (1) + ethanol (2) + extraction solvent (3); and b) heptane (1) + ethanol (2) + extraction solvent (3).

3.5. Simulation Results

The purification of hydrocarbons (hexane or heptane) from its azeotropic mixture by means of an extraction process is carried out in this work. The simulation study is a valuable tool in order to evaluate the possible implementation of this extraction process at industrial scale. Fig. 4 schematically illustrates the flowsheet studied in this work: a countercurrent continuous liquid-liquid extraction column and a solvent recovery stage. In this figure, the liquid-liquid extractor (with one equilibrium stage at 298.15 K and 101.32 kPa) models the liquid-liquid extraction column and the short-cut distillation models the solvent recovery stage. This extraction process was optimized via Aspen Hysys V.9 (Aspen Technology Inc., Cambridge, MA, USA). The parameters optimized with the NRTL model at 298.15 K were used to reproduce the phase behavior of the ternary systems hydrocarbon (1) + ethanol (2) + solvent (3). Operating conditions for the simulation study were selected to decrease the costs while respecting the requirement of an elevated raffinate purity. Both cost and purity increase when the ratio of the solvent/feed flow rise and the solvent purity increase. If this ratio is minimum, it will be possible to introduce a high quantity of azeotropic mixture consuming a minimum of solvent. Besides, the cost of solvent recovery increase when its purity is high. Based on this information, we have selected a solvent/feed ratio lower than 1.5 and a solvent stream of 80%. In these conditions, all solvent streams are liquid and are out of SLE region. Then, the liquid-liquid extractor can be used for the separations of these azeotropes. Then, the solvent recovered in the short-cut distillation unit was always 80%, feeding the liquid-liquid extractor unit. The feed (azeotropic mixture) and solvent compositions were kept constant and the flow rates were optimized to maximize raffinate purity.

The Table S7 of SI lists the properties of all streams in the extraction process used to separate ethanol from its azeotropic mixture. Moreover, a comparison between the data obtained for the

PILs studied in this work with the other extraction solvents used in the literature [10-18,25-37] is included in Figs. 5 and 6. In general, the ability of these solvents as an azeotrope breaker in extraction processes for the separation of the mixtures hydrocarbon + ethanol has been proved. Taking into account the results, the increment of the alkyl chain on cation and anion increases the purity of raffinate stream (hexane and heptane). These purities obtained in the separation of hexane + ethanol (≥80% in molar fraction) are higher than in the case of heptane + ethanol (see Fig. 5). The high ionicity ionic liquids (HIILs) [10,27] and deep eutectic solvents (DESs) [18,36,37] are more efficient in the heptane purification. The effect of the ionic liquid's cation nature can be studied using the bis(trifluoromelthylsulfonyl)imide-based ionic liquids where the hexane purity in the raffinate stream can be ranked as: $[C_4C_1Im] > [C_4C_1py] > [N_{1114}]$. The best performances in the separations of hydrocarbons from their mixtures with ethanol were achieved with $[C_4C_1pyr][N(CN)_2]$ in the case of hexane and with $[C_2C_1Im][C_1CO_2]$ in the case of heptane. In both separations ILs based on sulphate anion also revealed very good results.

Distillation of the extract stream affords the recovery of 80:20 solvent (recycled to the liquid-liquid extractor) and an ethanol stream containing different alcohol purities which are illustrated in Fig. 6. In this steam, similar results are obtained for both azeotropic mixtures hexane + ethanol and heptane + ethanol. In general, almost all extraction solvents achieve ethanol purities greater than 80%. The best ethanol purities were obtained through the DES 0.5 $[N_{1112(OH)}]Cl$ + 0.5 $[C_2H_2O_4]$ for hexane and using $[C_3C_1Im][N(CF_3SO_2)_2]$ for heptane.

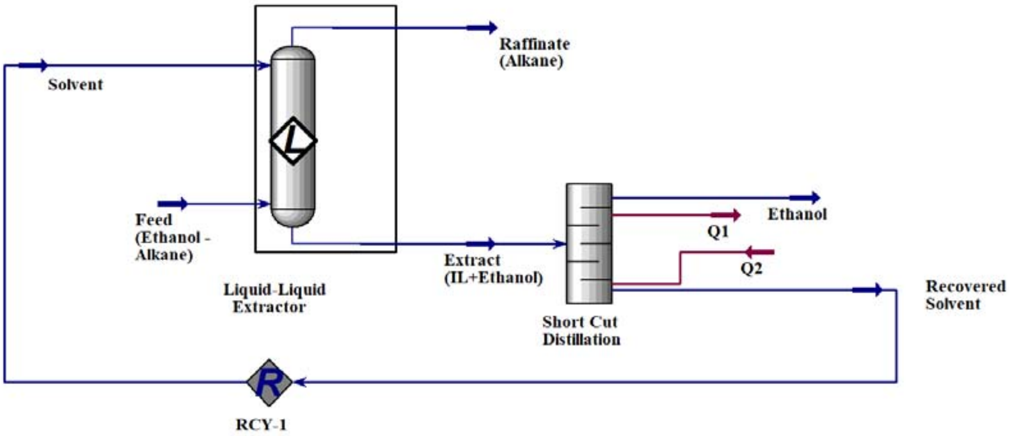

Fig. 4. Process flowsheet in the purification of hydrocarbons from its azeotropic mixture with ethanol.

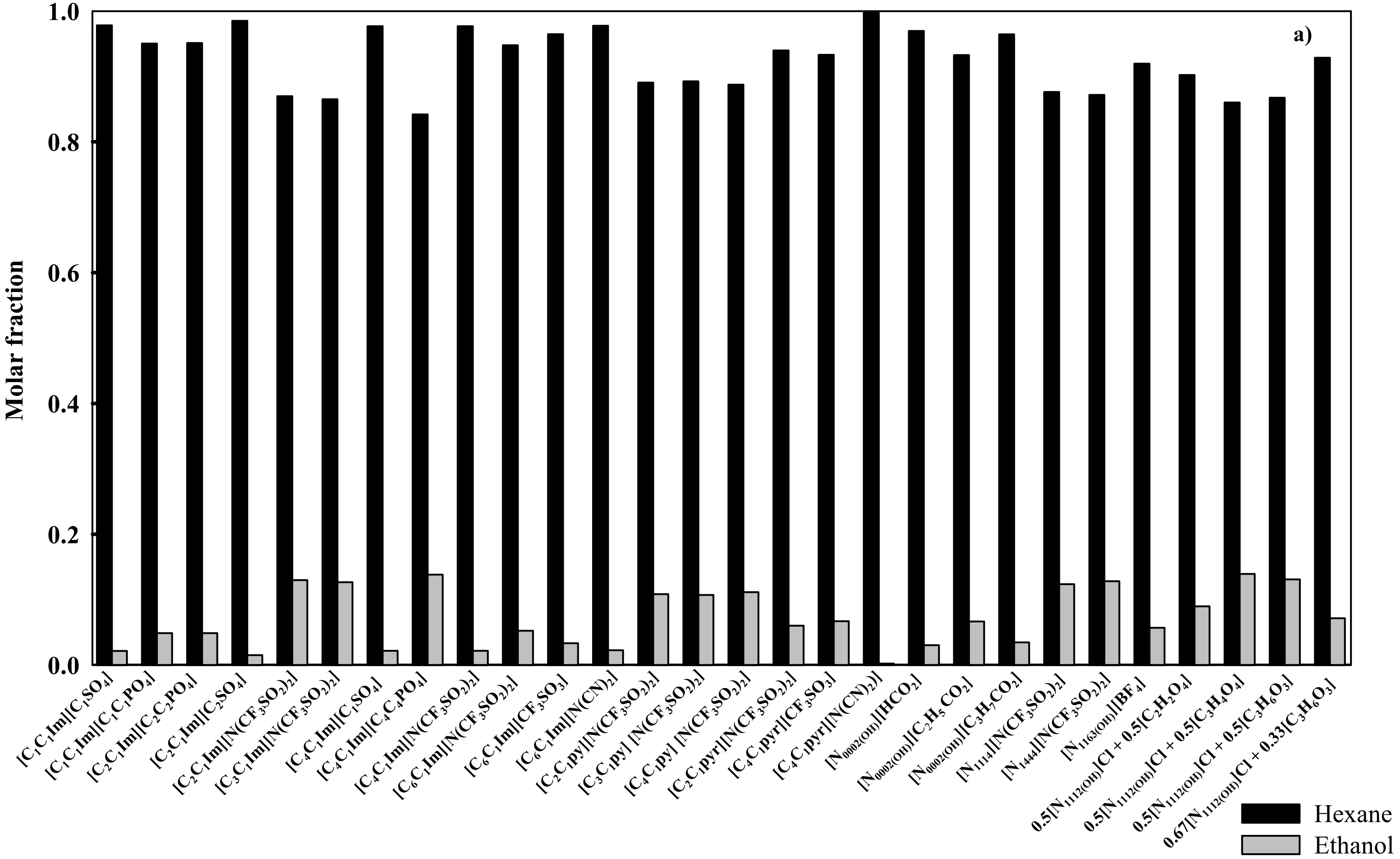
a)
Molar fraction
1.0
0.8
0.6
0.4
0.2
0.0
$[C_1C_1Im][C_1SO_4]$
$[C_1C_1Im][C_1C_1PO_4]$
$[C_2C_1Im][C_2C_2PO_4]$
$[C_2C_1Im][C_2SO_4]$
$[C_2C_1Im][N(CF_3SO_2)_2]$
$[C_3C_1Im][N(CF_3SO_2)_2]$
$[C_4C_1Im][C_1SO_4]$
$[C_4C_1Im][C_4C_4PO_4]$
$[C_4C_1Im][N(CF_3SO_2)_2]$
$[C_6C_1Im][N(CF_3SO_2)_2]$
$[C_6C_1Im][CF_3SO_3]$
$[C_6C_1Im][N(CN)_2]$
$[C_2C_1py][N(CF_3SO_2)_2]$
$[C_3C_1py] [N(CF_3SO_2)_2]$
$[C_4C_1py] [N(CF_3SO_2)_2]$
$[C_2C_1pyr][N(CF_3SO_2)_2]$
$[C_4C_1pyr][CF_3SO_3]$
$[C_4C_1pyr][N(CN)_2)]$
$[N_{0002(OH)}][HCO_2]$
$[N_{0002(OH)}][C_2H_5CO_2]$
$[N_{0002(OH)}][C_3H_7CO_2]$
$[N_{1114}][N(CF_3SO_2)_2]$
$[N_{1444}][N(CF_3SO_2)_2]$
$[N_{1163(OH)}][BF_4]$
$0.5[N_{1112(OH)}]Cl + 0.5[C_2H_2O_4]$
$0.5[N_{1112(OH)}]Cl + 0.5[C_3H_4O_4]$
$0.5[N_{1112(OH)}]Cl + 0.5[C_3H_6O_3]$
$0.67[N_{1112(OH)}]Cl + 0.33[C_3H_6O_3]$
Hexane
Ethanol

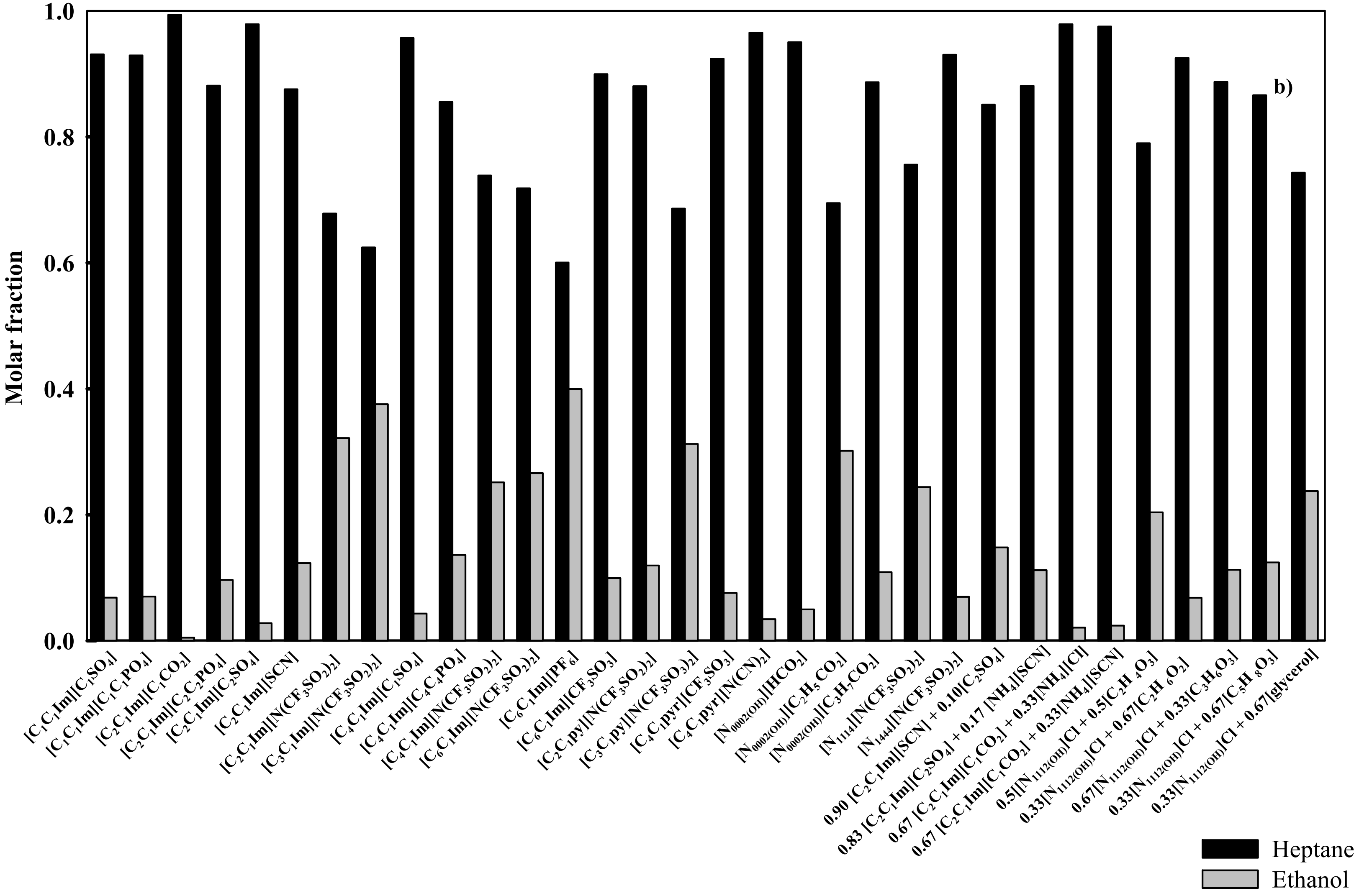

Fig. 5. Molar fraction of raffinate stream in the steady state calculated from simulations using Aspen Hysys for the purification of: a) hexane; and b) heptane.

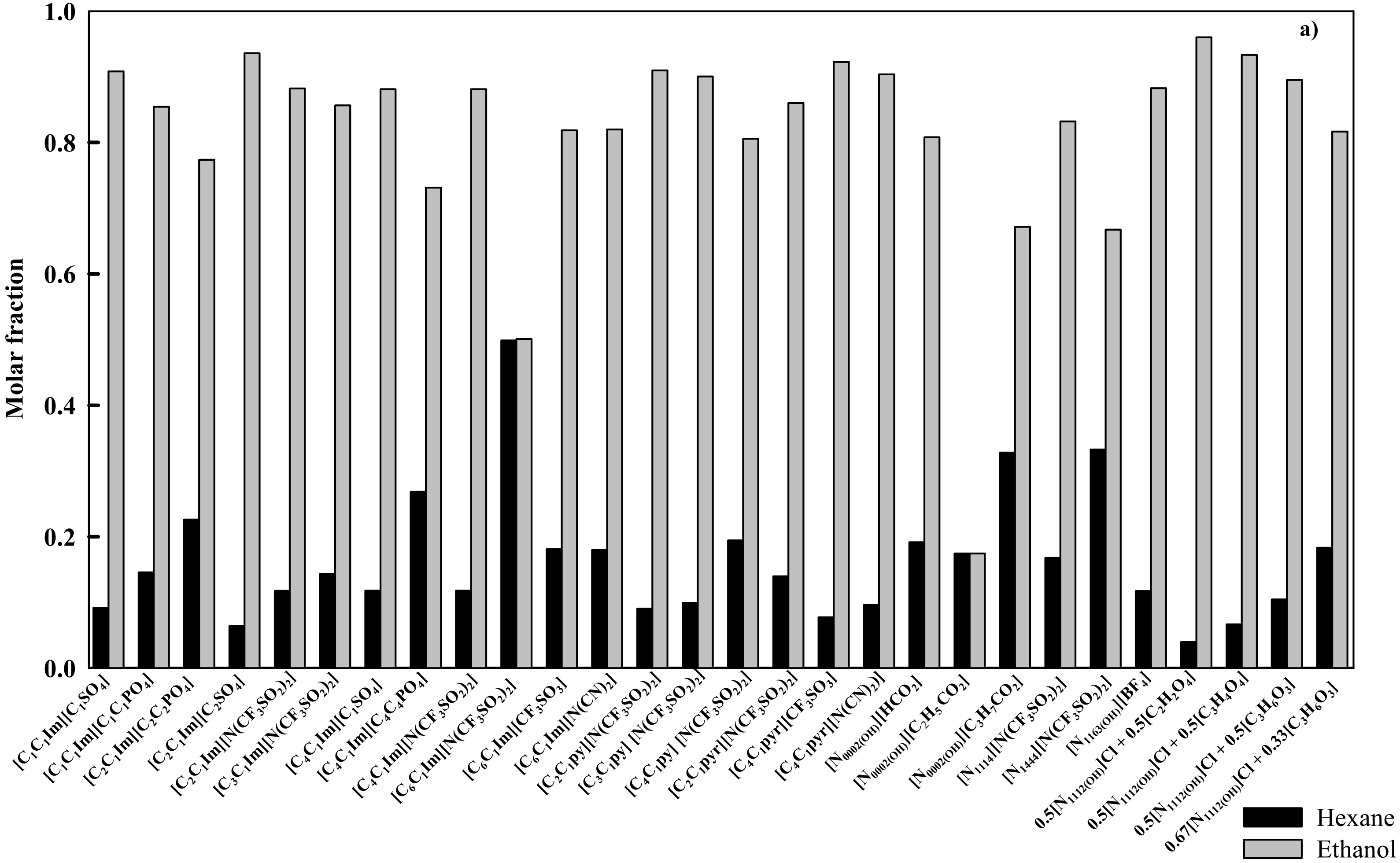
a)
Molar fraction
1.0
0.8
0.6
0.4
0.2
0.0
$[C_1C_1Im][C_1SO_4]$
$[C_1C_1Im][C_1C_1PO_4]$
$[C_2C_1Im][C_2C_2PO_4]$
$[C_2C_1Im][C_2SO_4]$
$[C_2C_1Im][N(CF_3SO_2)_2]$
$[C_3C_1Im][N(CF_3SO_2)_2]$
$[C_4C_1Im][C_1SO_4]$
$[C_4C_1Im][C_4C_4PO_4]$
$[C_4C_1Im][N(CF_3SO_2)_2]$
$[C_6C_1Im][N(CF_3SO_2)_2]$
$[C_6C_1Im][CF_3SO_3]$
$[C_6C_1Im][N(CN)_2]$
$[C_2C_1py][N(CF_3SO_2)_2]$
$[C_3C_1py] [N(CF_3SO_2)_2]$
$[C_4C_1py] [N(CF_3SO_2)_2]$
$[C_2C_1pyr][N(CF_3SO_2)_2]$
$[C_4C_1pyr][CF_3SO_3]$
$[C_4C_1pyr][N(CN)_2)]$
$[N_{0002(OH)}][HCO_2]$
$[N_{0002(OH)}][C_2H_5CO_2]$
$[N_{0002(OH)}][C_3H_7CO_2]$
$[N_{1114}][N(CF_3SO_2)_2]$
$[N_{1444}][N(CF_3SO_2)_2]$
$[N_{1163(OH)}][BF_4]$
$0.5[N_{1112(OH)}]Cl + 0.5[C_2H_2O_4]$
$0.5[N_{1112(OH)}]Cl + 0.5[C_3H_4O_4]$
$0.5[N_{1112(OH)}]Cl + 0.5[C_3H_6O_3]$
$0.67[N_{1112(OH)}]Cl + 0.33[C_3H_6O_3]$
Hexane
Ethanol

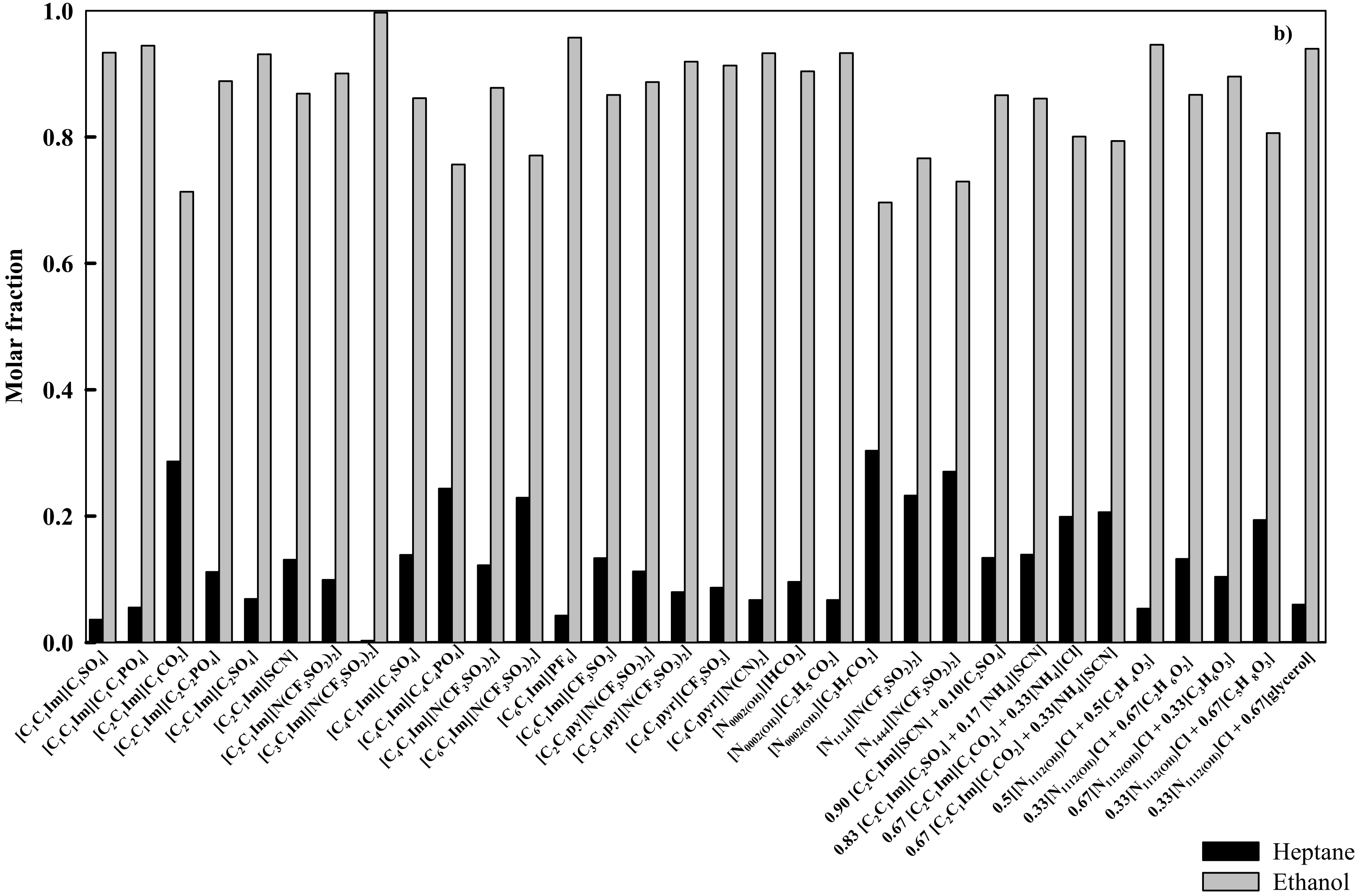

Fig. 6. Molar fraction of ethanol stream in the steady state calculated from simulations using Aspen Hysys for the purification of: a) hexane; and b) heptane.

4. Conclusion

In this work, a series of protic ionic liquids based on 2-hydroxyethylamonium cation were evaluated to extract ethanol from its azeotropic mixture with hydrocarbons (hexane and heptane). These PILs were synthesized and several thermodynamic and thermophysical properties were measured at atmospheric pressure and different temperatures. Experimental LLE data were determined at 298.15 K and these data were used to identify the theoretical operation conditions for extraction process. The corresponding distribution ratios and selectivities were determined. NRTL model was used to correlate these experimental LLE data. The parameters calculated from NRTL model allow the implementation and use in simulation studies for the design of extraction process. The design of a countercurrent continuous extraction process including a solvent recycling stage was optimized using a conventional software. The results obtained with the different extraction solvents used in this work and in the literature demonstrate the efficiency of this extraction process for the purification of hydrocarbons (hexane and heptane) from its azeotropic mixture with ethanol. Taking into account the raffinate purities obtained in these studies, scaling up for industrial applications can be viable. In this work, liquid-liquid extraction process was proposed as alternative to azeotropic or extractive distillation because it can be more environmentally friendly separation process. This separation process is preferred from the economical point of view because the energy requirement is much lower than conventional processes.

5. Acknowledgements

Financial support from FCT/MEC (Portugal), through Investigador FCT 2014 (IF/00190/2014 to A.B.P and IF/00210/2014 to J.M.M.A.) and projects PTDC/EQU-EQU/29737/2017, PTDC/QEQ-FTT/3289/2014 and IF/00210/2014/CP1244/CT0003. This work was also supported by the Associate Laboratory for Green Chemistry LAQV (financed by national funds from FCT/MCTES (UID/QUI/50006/2019)) and co-financed by the ERDF under the PT2020 Partnership Agreement (POCI-01-0145-FEDER - 007265). Eliseo Amado-González wants to thank the financial support of University of Pamplona, Internal Project 2-2017.

6. References

[1] R. I. Canales, J.F. Brennecke, Comparison of ionic liquids to conventional organic solvents for extraction of aromatics from aliphatics, J. Chem. Eng. Data 61 (2016) 1685-1699.

[2] A. B. Pereiro, A. Rodríguez, Mixing properties of binary mixtures presenting azeotropes at several temperatures, J. Chem. Thermodyn. 39 (2007) 1219-1230.

[3] M. J. Earle, J. M. S. S. Esperança, M. Gilea, J. N. C. Lopes, L. P. N. Rebelo, J. W. Magee, J. Widegren, The distillation and volatility of ionic liquids, Nature 439 (2006) 831-834.

[4] R. D. Rogers, K. R. Seddon, Ionic Liquids - Solvents of the Future, Science 302 (2003) 792-794.

[5] J. G. Huddleston, A. E. Visser, W. M. Reichert, H. D. Willauer, G. A. Broker, R. D. Rogers, Characterization and comparison of hydrophilic and hydrophobic room temperature ionic liquids incorporating the imidazolium cation, Green Chem. 3 (2001) 156–164.

[6] N. V. Plechkova, K. R. Seddon, Applications of ionic liquids in the chemical industry, Chem. Soc. Rev. 37 (2008) 123-150.

[7] J. N. Canongia, J. M. S. S. Esperança, A. Mão de Ferro, A. B. Pereiro, N. V. Plechkova, L. P. N. Rebelo, K. R. Seddon, I. Vázquez-Fernández, Protonic Ammonium Nitrate Ionic Liquids and Their Mixtures: Insights into Their Thermophysical Behaviour, J. Phys. Chem. B 120 (2016) 2397-2406.

[8] N. Bicak, A new ionic liquid: 2-hydroxy ethylammonium formate, J. Mol. Liq. 116 (2005) 15-18.

[9] S. M. Hosseini, M. M. Alavianmehr, A. Gutiérrez, R. Khalifeh, J. Moghadasi, S. Aparicio, On the properties and structure of 2-hydroxyethylammonium formate ionic liquid, J. Mol. Liq. 249 (2018) 233-244.

[10] F. S. Oliveira, R. Dohrn, A. B. Pereiro, J. Araujo, L. P. Rebelo, I. M. Marrucho, Designing high ionicity ionic liquids based on 1-ethyl-3-methylimidazolium ethyl sulphate for effective azeotrope breaking, Fluid Phase Equilib. 419 (2016) 57-66.

[11] A. B. Pereiro, A. Rodriguez, J. Canosa, J. Tojo, Ionic liquid that separates the azeotropic mixture ethanol HMImPF$_6$, Green Chem. 8 (2006) 307-310.

[12] A. B. Pereiro, A. Rodriguez, Purification of hexane with effective extraction using ionic liquid as solvent, Green Chem. 11 (2009) 346-350.

[13] A. B. Pereiro, A. Rodriguez, Separation of ethanol-heptane azeotropic mixtures by solvent extraction with an ionic liquid, Ind. Eng. Chem. Res. 48 (2009) 1579-1585.

[14] A. B. Pereiro, A. Rodríguez, Azeotrope-breaking using [BMIM] [MeSO4] ionic liquid in an extraction column, Sep. Purif. Technol. 62 (2008) 733-738.

[15] A. B. Pereiro, A. Rodríguez, Effective extraction in packed column of ethanol from the azeotropic mixture ethanol+hexane with an ionic liquid as solvent, Chem. Eng. J. 153 (2009) 80-85.

[16] A. B. Pereiro, F. J. Deive, J. M. S. S. Esperança, A. Rodríguez, Alkylsulfate-based ionic liquids to separate azeotropic mixtures, Fluid Phase Equilib. 291 (2010) 13-17.

[17] P. D. Bastos, F. S. Oliveira, L. P. N. Rebelo, A. B. Pereiro, I. M. Marrucho, Separation of azeotropic mixtures using high ionicity ionic liquids based on 1-ethyl-3-methylimidazolium thiocyanate, Fluid Phase Equilib. 389 (2015) 48-54.

[18] F. S. Oliveira, A. B. Pereiro, L. P. N. Rebelo, I. M. Marrucho, Deep eutectic solvents as extraction media for azeotropic mixtures, Green Chem. 15 (2013) 1326-1330.

[19] A. B. Pereiro, A. Rodriguez, A study on the liquid-liquid equilibria of 1-alkyl-3-methylimidazolium hexafluorophosphate with ethanol and alkanes, Fluid Phase Equilib. 25 (2008) 23-29.

[20] L. Laroche, N. Bekiaris, H. W. Andersen, M. Morari, Homogeneous Azeotropic Distillation: Comparing Entrainers. Can, J. Chem. Eng. 69 (1991) 1302–1319.

[21] S. J. Marwil, Separation of hydrocarbon and alcohol azeotropic mixtures by distillation with anhydrous ammonia, U.S. Patent 4437941, March 1984.

[22] T. Okada, T. Matsuura, A study on the pervaporation of ethyl alcohol/heptane mixtures by porous cellulose membranes, Proc. Int. Conf. Pervaporation Processes Chem. Ind. 3rd (1988) 224–230.

[23] M. Laatikainen, M. Lindstrom, Separation of methanol-ethanol and ethanol-normal-heptane mixtures by reverse-osmosis and pervaporation. Acta Polytech Scandinavica Chem. Tech. Metall. 175 (1986) 1-61.

[24] H. Renon, J. Prausnitz, Local compositions in thermodynamic excess functions for liquid mixtures, AIChE J. 14 (1968) 135-144.

[25] F. Cai, M. Zhao, Y. Wang, F. Wang, G. Xiao, Phosphoric-based ionic liquids as solvents to separate the azeotropic mixture of ethanol and hexane, J. Chem. Thermodyn. 81 (2015) 177-183.

[26] F. Cai, G. Xiao, Liquid–liquid equilibria for ternary systems ethanol + heptane + phosphoric-based ionic liquids, Fluid Phase Equilib. 386 (2015) 155-161.

[27] F. S. Oliveira, R. Dohrn, L. P. Rebelo, I. M. Marrucho, Improving the separation of n-heptane + ethanol azeotropic mixtures combining ionic liquid 1-ethyl-3-methylimidazolium acetate with different inorganic salts, Ind. Eng. Chem. Res. 55 (2016) 5965-5972.

[28] S. Corderí, B. González, Ethanol extraction from its azeotropic mixture with hexane employing different ionic liquids as solvents, J. Chem. Thermodyn. 55 (2012) 138-143.

[29] R. Seoane, E. González, E. Gonzalez, 1-Alkyl-3-methylimidazolium bis(trifluoromethylsulfonyl)imide ionic liquids as solvents in the separation of azeotropic mixtures, J. Chem. Thermodyn. 53 (2012) 152-157.

[30] S. Corderí, B. González, N. Calvar, E. Gómez, Ionic liquids as solvents to separate the azeotropic mixture hexane/ethanol, Fluid Phase Equilib. 337 (2013) 11-17.

[31] W. Liu, Y. Ri, K. Ma, X. Xu, Z. Zhu, Y. Wang, Application of 1-hexyl-3-methylimidazolium trifluoromethanesulfonate to the removal of alcohol from mixtures with heptane, Fluid Phase Equilib. 443 (2017) 44-49.

[32] B. González, S. Corderí, A. Santamaria, Application of 1-alkyl-3-methylpyridinium bis(trifluoromethylsulfonyl)imide ionic liquids for the ethanol removal from its mixtures with alkanes, J. Chem. Thermodyn. 60 (2013) 9-14.

[33] B. González, S. Corderí, Capacity of two 1-butyl-1-methylpyrrolidinium-based ionic liquids for the extraction of ethanol from its mixtures with heptane and hexane, Fluid Phase Equilib. 354 (2013) 89-94.

[34] N. M. Aranda, B. González, Cation effect of ammonium imide based ionic liquids in alcohols extraction from alcohol-alkane azeotropic mixtures, J. Chem. Thermodyn. 68 (2014) 32-39.

[35] U. Domanska, Z. Zołek-Tryznowska, A. Pobudkowska, Separation of hexane/ethanol mixtures. LLE of ternary systems (ionic liquid or hyperbranched polymer + ethanol + hexane) at T = 298.15 K, J. Chem. Eng. Data 54 (2009) 972-976.

[36] A. A. Samarov, M. A. Smirnov, M. P. Sokolova, E. N. Popova, A. M. Toikka, Choline chloride based deep eutectic solvents as extraction media for separation of n-hexane + ethanol mixture, Fluid Phase Equilib. 448 (2017) 123-127.

[37] N. R. Rodriguez, B. Molina, M. C. Kroon, Aliphatic + ethanol separation via liquid–liquid extraction using low transition temperature mixtures as extracting agents, Fluid Phase Equilib. 394 (2015) 71-82.

[38] B. Janković, N. Manić, R. Buchner, I. P. Korus, A. B. Pereiro, E. A. González, Dielectric spectroscopy and kinetic analysis of nonisothermal decomposition of ionic liquids derived from organic acid, Thermochim. Acta 672 (2019) 46-52.

[39] A. Pinkert, K. L. Ang, K. N. Marsh, S. Pang, Density, viscosity and electrical conductivity of protic alkanolammonium ionic liquids, Phys. Chem. Chem. Phys. 13 (2011) 5136-5143.

[40] R. Olmos, I. Cota, M. Iglesias, F. Medina, New short aliphatic chain ionic liquids: synthesis, physical properties, and catalytic activity in aldol condensations, J. Phys. Chem. 111 (2007) 12468-12477.

[41] M. H. Ghatee, M. Bahrami, N. Khanjari, H. Firouzabadi, Y. Ahmadi, A functionalized high-surface-energy ammonium-based ionic liquid: experimental measurement of viscosity, density, and surface tension of (2-hydroxyethyl)ammonium formate, J. Chem. Eng. Data 57 (2012) 2095-2101.

[42] M. Iglesias, A. Torres, R. Gonzalez-Olmos, D. Salvatierra, Effect of temperature on mixing thermodynamics of a new ionic liquid: {2-Hydroxy ethylammonium formate (2-HEAF) + short hydroxylic solvents}, J. Chem. Thermodyn. 40 (2008) 119-133.

[43] F. M. Mesquita, R. S. Pinheiro, R. S. Aguiar, H. B. Sant'Ana, Measurement of phase equilibria data for the extraction of toluene from alkane using different solvents, Fluid Phase Equilib. 404 (2015) 49-54.

[44] X. L. Yuan, S. J. Zhang, X. M. Lu, Hydroxyl ammonium ionic liquids: synthesis, properties, and solubility of SO_2, J. Chem. Eng. Data 52 (2007) 596-599.

[45] A. A. Samarov, M. A. Smirnov, M. P. Sokolova, E. N. Popova, A. M. Toikka, Choline chloride based deep eutectic solvents as extraction media for separation of n-hexane + ethanol mixture, Fluid Phase Equilib. 448 (2017) 123-127.

[46] A. Marcilla, M. M. Olaya, M. D. Serrano, Comments on Liquid-Liquid Equilibrium Data Regression, J. Chem. Eng. Data 52 (2007) 2538-2541.

[47] A. Marcilla, J. A. Reyes-Labarta, M. M. Olaya, Should we trust all the published LLE correlation parameters in phase equilibria? Necessity of their assessment prior to publication, Fluid Phase Equilib. 433 (2017) 243-252.

[48] I. Díaz, M. Rodríguez, E. J. González, M. González-Miquel, A simple and reliable procedure to accurately estimate NRTL interaction parameters from liquid-liquid equilibrium data, Chem. Eng. Sci. 193 (2019) 370-378.